# Phosphate Positioning and Availability in the Starch Granule Matrix as Studied by EPR

Andreas Blennow,*,† Karen Houborg,† Roger Andersson,‡ Ewa Bidzińska,§ Krystyna Dyrek,|| and Maria Łabanowska||

*Center for Molecular Plant Physiology, Department of Plant Biology, The Royal Veterinary and Agricultural University, 40 Thorsvaldsensvej, DK 1871 Frederiksberg C. Copenhagen, Denmark, Department of Food Science, Swedish University of Agricultural Science, P.O. Box 7051, SE-750 07 Uppsala, Sweden, Regional Laboratory of Physicochemical Analyses and Structural Research, Ingardena 3, 30-060 Cracow, Poland, and Faculty of Chemistry, Jagiellonian University, Ingardena 3, 30-060 Cracow, Poland*

*Received December 1, 2005; Revised Manuscript Received January 16, 2006*

$Cu^{2+}$ was introduced as an EPR probe into the starch granules isolated from different starch crop genotypes including transgenically modified potatoes generated for extreme amylose and starch phosphate monoester concentrations. Several discrete copper adducts bound to the starch matrix with different strength was revealed. It was found that phosphate has a significant influence on the type of these species, their number, location in the structure, and strength of binding. Well dispersed $Cu^{2+}$ complexes with axial symmetry are formed in the semicrystalline part of the starch linked through O−P− bonds in the phosphorylated starches. In the amorphous part of the starch, freely rotating hexaaqua complexes of $Cu^{2+}$ and complexes coupled antiferromagnetically are formed. The amount of the former increases with content of phosphate indicating enhanced binding of water in the granules. The results complement previous experimental data and molecular models for the starch granule with respect to the location and effects of phosphate and crystalline matter.

## Introduction

Starch is the only significant crystalline intracellular biopolymer in the living cell. It is also a dominating carbohydrate polymer on earth, and its abundance and quality makes starch interesting for a number of food and material applications.[1] The well ordered structure of starch and the presence in most of the native starches of phosphate groups renders starch a position as a potential raw material for the development of future renewable nano materials, crystalline conducting polymers, etc. The reason for its semicrystalline and well-ordered structure is the repetitive structure of α-D-glucose residues linked by two types of bonds: α-1,4 and α-1,6 glucosidic linkages. The major polysaccharides of starch granules are amylopectin and amylose. Amylopectin (typically ∼75%) is a semicrystalline highly branched polysaccharide with an α-1,4 glucosidic backbone and 4−5% α-1,6 branch points, whereas amylose (typically ∼25%) is amorphous in the native starch granule and is composed of essentially linear chains of α-1,4 linked glucose units. Despite the quite trivial chemical composition of starch polysaccharides, the starch molecules in the final native starch granule are folded and assembled in complex structures, though interesting constant features are evident. A storage starch granule appears as a semicrystalline entity, up to 100 μm in length.[2] For granules larger than approximately 1 μm, the α-1,6 branch points in the amylopectin facilitate the formation of parallel double helical segments that align radially in the granule forming arrays of quasiconcentric lamellae with a constant 9 nm repeat as determined by small-angle X-ray spectroscopy (SAXS).[3] The 2−4 nm thick base of a lamella contains most of the α-1,6 branch points and therefore considered amorphous whereas the 5−7 nm double helical segments extending from the branch points are considered as highly crystalline and register in different types of crystalline polymorphs.[4,5]

Starches extracted from almost all plant genotypes and plant organs are phosphorylated.[6] However, the concentration of phosphate is low (approximately 0.1−50 nmoles/mg starch) and varies considerably with the genotype of the starch storing organism.[7,8] It is since long documented[9] that the majority of the phosphate groups in starch is covalently bound to amylopectin but not to the same extent to amylose. More detailed investigations have demonstrated that the phosphate groups are bound as monoesters at the C-6 and the C-3 position of the glucose units.[10−13] The ratio of C-3 and C-6 substituted hydroxyl groups ranges from 2:3[11] to 1:10.[14] It has also been documented for starches extracted from several genotypes that the phosphorylated chains are considerably longer than the average length of the nonsubstituted chains.[7,13−15] This seems to be a direct effect of the substrate specificity of the starch phosphorylating enzyme, GWD (glucan water dikinase).[16] A recent particle-induced X-ray emission (PIXE) study[17] indicates that the phosphate groups are located throughout the starch granule matrix however somewhat more concentrated to the center of the granule. Analysis of starch granules after selective long term hydrolysis of the amorphous parts of the starch granule yielding highly crystalline dextrins representing the crystalline lamellae suggests that both crystalline (double helical lamellar) and amorphous (branched sections or unregistered double helices) amylopectin regions contain esterified phosphate.[18] The free C-3 and C-6 hydroxyl groups of the glucose units are located at the hydrophilic surface of the double helix, implying that phosphate groups protrude from the helix surface, suggesting that stability

* To whom correspondence should be addressed. Tel: +4535283334. Fax: +4535283333. E-mail: abl@kvl.dk.

† The Royal Veterinary and Agricultural University.

‡ Swedish University of Agricultural Science.

§ Regional Laboratory of Physicochemical Analyses and Structural Research.

|| Jagiellonian University.

10.1021/bm050919g CCC: $33.50 
Published on Web 02/16/2006

**Table 1.** Starch Samples and Treatments with $CuCl_2$[a]

| sample | 1 | 2 | 3 | 4 | 5 | 6 | 7 |
|---|---|---|---|---|---|---|---|
| normal maize | no $Cu^{2+}$ | $Cu^{2+}$ eq x 1 | $Cu^{2+}$ eq x 2 | $Cu^{2+}$ eq x 3 | $Cu^{2+}$ eq x 5 | no. 5 annealed at 80°C | no. 5 lintnerized |
| LP potato | no $Cu^{2+}$ | $Cu^{2+}$ eq x 1 | $Cu^{2+}$ eq x 2 | $Cu^{2+}$ eq x 3 | $Cu^{2+}$ eq x 5 | no. 5 annealed at 60°C | no. 5 lintnerized |
| Normal potato | no $Cu^{2+}$ | $Cu^{2+}$ eq x 1 | $Cu^{2+}$ eq x 2 | $Cu^{2+}$ eq x 3 | $Cu^{2+}$ eq x 5 | no. 5 annealed at 55°C | no. 5 lintnerized |
| HAP potato | no $Cu^{2+}$ | $Cu^{2+}$ eq x 1 | $Cu^{2+}$ eq x 2 | $Cu^{2+}$ eq x 3 | $Cu^{2+}$ eq x 5 | no. 5 annealed at 65°C | no. 5 lintnerized |
| *C. zedoaria* | no $Cu^{2+}$ | $Cu^{2+}$ eq x 1 | $Cu^{2+}$ eq x 2 | $Cu^{2+}$ eq x 3 | $Cu^{2+}$ eq x 5 | no. 5 annealed at 67°C | no. 5 lintnerized |

[a] LP: Low phosphate, HAP: high amylose and phosphate, samples numbered 1 were not incubated with copper. Samples numbered 2 were treated with copper and equilibrated (eq) once with water ($Cu^{2+}$ eq x 1), samples numbered 3 were equilibrated twice with water ($Cu^{2+}$ eq x 2) etc. (see Materials and Methods).

of packing of the helices may be affected. Such effects have been indicated by differential scanning calorimetry (DSC)[19,20] and by X-ray crystallography.[21] Extending molecular models[22] to include the phosphate group in the double helix motif suggests that the C-6 positioned phosphate groups appear to be able to align well in one of the double helix surface grooves.[23] As a consequence these phosphate groups would possibly not affect either double helix formation or the inter-helical crystalline packing. C-3 phosphate groups are expected to be more exposed at the helix surface.[6] Hence, further studies are needed to better clarify the effects of differently positioned phosphate groups in the starch granule matrix.

Genetic engineering strategies of starch crops have resulted in the generation of a variety of starch types having fundamentally different and sometimes extreme functionalities.[24] Specific strategies have been outlined for the engineering of phosphorylation of starch.[6] It is well-known that the presence of phosphate groups in starch increases the hydration capacity of starch pastes upon disruption and gelatinization of the native starch granules in aqueous media, and as a result, the starch phosphate content is correlated to starch paste peak viscosity, swelling, and gel forming capacity.[25,26] However, the distributional positioning and more precise effects of phosphate in the native starch granule are questions still open for debate.

In this investigation, electron paramagnetic resonance (EPR) spectroscopy was used to gain additional information on the influence of phosphate on specific structures of the native starch granule. The EPR technique is commonly used for studying paramagnetic centers. In bioorganic materials EPR is mostly applied for detection of free radicals created upon irradiation with $\gamma$-, UV-[27,28] or by thermal treatment.[29,30] In the case of organic polymers, transition metal ions incorporated into the structure may be used as paramagnetic probes revealing the features of the hosting material.[31−33] The latter approach with paramagnetic $Cu^{2+}$ ions as a probe was used in the present work. The copper ions were introduced into the starch as $CuCl_2$ water solutions, i.e., in the form of $[Cu(H_2O)_6]^{2+}$ and/or $[Cu(H_2O)_xCl_y]^{(2-y)+}$ species. As a result of interaction of such complexes with the starch matrix, formation of bonds may occur between $Cu^{2+}$ central ions and the terminal hydroxyl groups of the glucose units and/or phosphate monoesters covalently linked to the starch.

The $Cu^{2+}$ ions were introduced into starches with wild genotypes type as well as starches genetically engineered for altered phosphate and glucan chain length[25,34] and starch samples that were chemically or physically treated. The type of copper complexes formed was investigated by EPR. Computer simulation was applied to obtain the best fit between experimental and calculated EPR spectra, which enabled insight into the formation of particular species, depending on the type of the starch and the concentration of phosphate. Gradual equilibration of the samples with added portions of water provided data on the accessibility of these species in the starch granule and the strength of their binding by the starch matrix. The data support that phosphate esters are present as discrete species in the starch granule matrix and that phosphate significantly affects matrix hydration properties.

## Experimental Section

**Materials.** *Generation and Isolation of Starches.* High amylose and phosphate (HAP) potato starch was produced using a genetic engineering approach by the antisense suppression of the two starch branching enzyme isoforms in potato c.v. "Dianella".[34,35] Low phosphate (LP) potato starch was generated using the same strategy by the antisense suppression of the starch phosphorylating enzyme glucan water dikinase (GWD) in potato c.v. "Dianella".[25] Starch granules were gently extracted and purified from mature and fresh potato tubers and from rhizomes of *Curcuma zedoaria* using the method described.[14] Normal potato starch c.v. "Kuras" was provided by Kartoffelmelcentralen (KMC) Denmark and normal maize starch was provided by Cerestar AKV I/S, Denmark.

Five samples of starch with different phosphate and amylose contents and amylopectin chain lengths were investigated: normal maize, LP potato, normal potato, HAP potato, and *C. zedoaria*. The notation of the samples is given in Table 1. To fully protonise the phosphate groups, a 1 g portion of each starch was equilibrated three times in 15 mL of 10 mM HCl and then washed until neutral with double deionized water. Portions of 1 g of the starch samples were subsequently equilibrated twice for 10 min with 1 M $CuCl_2$, and excess $CuCl_2$ solution was removed. Different concentrations of copper in the starch samples was achieved by addition of 10 mL of double deionized water to each 1 g sample of copper treated starch suspension, allowing the suspension to reach equilibrium and settle, and thereafter, the excess liquid was discarded. Decreasing concentration of copper in the starches until constant levels was reached by repeating the water washing procedure (Table 1). All starch samples were allowed to air-dry at room temperature.

**Methods.** *Preparation of Lintner Starches and Starch Annealing.* Highly crystalline Lintner starches were prepared using the rapid method as described[36] and modified.[18] Annealing was performed in excess water for 30 min at 5 °C below the gelatinization point as determined by differential scanning calorimetry (DSC).[37]

*Starch Analysis.* The concentration of amylose in the different starch types was determined specroscopically using iodine colorimetry as described.[11] The method is based on the significant difference in iodine binding capacity and spectral properties of the amylopectin and the amylose−iodine complexes, respectively. The ratio between amylose and amylopectin in the gelatinized starch samples was calculated from the absorbances at 550 and 620 nm, respectively, using pure potato amylopectin and amylose (Sigma) as standards. The analysis of the amylopectin chain length distribution by BioLC high performance anionic exchange chromatography (HPAEC) following amylopectin enzymatic debranching was carried out as described.[14] Briefly, purified starch (5 mg) was dissolved by heating in 1 mL of water and enzymically debranched using isoamylase (Megazyme, Sydney, Australia). Analysis of the liberated linear oligosaccharides was performed using a (Dionex DX 500) system equipped with a CarboPac PA-100

column and equipped with an S-3500 auto sampler, a GP40 pump, and an ED40 pulsed amperometric detector (PAD). Samples of 30 $\mu$L (150 $\mu$g of α-glucan), prepared as described above, were injected and separated using 1 mL/min flow rate and an isocratic NaOH and NaOAc gradient profile as specified.[11] Chromatograms were integrated using the Chromelion software (Dionex) corrections were made for deviations in detector response and the mean chain length was calculated for chains between DP (degree of polymerization) 6−60. Monoesterified phosphate was analyzed as the concentration of Glc-6-P using and enzyme linked assay following complete acid hydrolysis by the method of Bay-Smidt et al., (1994).[11] Total starch bound phosphate including the content of Glc-3-P was calculated from NMR data[18] on the basis that the wild-type Dianella starch having the constant C6:C3 = 2.53 substitution ratio independent of genetic modulation of the total phosphate content in the tubers. The concentration of copper and phosphate in the starch and Lintner samples was analyzed by ICP-AES as described below.

*ICP-AES.* Inductively coupled plasma-atomic emission spectroscopy (ICP-AES) analysis was carried out using a Perkin-Elmer Optima 3000 DV equipped with a Perkin-Elmer autosampler AS-91 (Perkin-Elmer corp., Norwalk, CT., USA). The ICP-AES instrument parameters with Hildebrand grid nebulizer and a quartz double-pass spray chamber were set to: frequency: 40 MHz, temperature, 8000 °C, coolant gas (argon) flow rate: 15 l/min, auxiliary gas (argon) flow rate: 0.3 l/min, nebulizer pressure: 45 psi, RF power: 1.3 kW. One g of starch (two replicates) was boiled with 30 mL of concentrated $HNO_3$ and the sample was diluted with water to a final volume of 100 mL. The results were calculated with the ICP Winlab software (version 1.2).

**EPR Measurements.** The EPR measurements were performed with a Bruker ELEXSYS 500 spectrometer (Karlsruhe, Germany) operating in X-band (9.2 GHz) at a modulation frequency of 100 kHz. The EPR spectra were recorded with modulation amplitude 1 mT and microwave power 10 mW at room (293 K) and liquid-nitrogen (77 K) temperatures. Measurements at low temperatures lead to better resolution of the EPR spectra and also can indicate the kind of interactions between paramagnetic species. The number of spins in the investigated samples was determined by comparison of the integral signal intensity of the investigated samples, obtained by double integration of the first derivative EPR signals, with that of a standard. Two different standards, containing coupled or isolated $Cu^{2+}$ species, were used: $CuSO_4 \cdot 5H_2O$, diluted with diamagnetic $K_2SO_4$, containing $5 \times 10^{19}$ spins/g or *C. zedoaria* Lintners with $Cu^{2+}$ ions content equal to $1.4 \times 10^{18}$ spins/g. The number of spins in the reference materials was determined by the analytical methods, independent of EPR.[38] All necessary precautions were followed in order to ensure good precision of the quantitative EPR measurements. These requirements concern "matching" of EPR parameters of the investigated samples and the standard (line shape, line width, spin concentration) and the same experimental conditions (modulation amplitude, power level, filling factor, temperature, etc.) of the recording of their EPR spectra.[38−40] EPR parameters of the investigated samples (*g* factor values: $g_{\parallel}$, $g_{\perp}$, and $g_{av}$; peak-to-peak line widths $\Delta B_{pp}$; hyperfine splitting constants: $A_{\parallel}$, $A_{\perp}$, integral intensities of the EPR signals) give information on the structure of paramagnetic centers, nature of binding between central ions and neighboring atoms, the number of paramagnetic species, and the kind of their mutual interactions. All of these parameters were determined by simulation, using EPR Program SIM14.[41] The original program was modified[42] by introducing a users' interface and optimization procedures. Simulation of the experimental EPR spectrum consists of its deconvolution into component signals and finding proportions in which particular components participate in the overall spectrum. The conclusive criterion of correct simulation is good fitting of the simulated spectrum to the experimental one.

## Results and Discussion

**Origin, Molecular Structure, and Chemical Composition of Starches.** For this study, starches derived from five different plant genotypes were selected on the basis of variations in specific structures, amylose concentration, amylopectin chain length profile, and the concentration of monoesterified phosphate (Table 2). Annealed starch, starch dehydrated at 120 °C, and starch samples in which the amorphous parts were removed by acid hydrolysis (Lintners) were also included. The higher phosphate concentrations found in the maize lintner compared to the native maize starch are a result of the presence of phospholipids specific for maize starch.

**Table 2.** Molecular Structures of the Starch Samples[a]

| sample | P in starch (nmol/mg starch)[b] | P in lintner (nmol/mg starch)[c,d] | amylose (%, w/w) | amylopectin mean chain length (DP) |
|---|---|---|---|---|
| normal maize | 0.08[d] | 0.5 | 45.3 (0.8) | 24.1 (0.1) |
| LP potato | 3.1 (0.3) | 2.9 | 37.5 (0.6) | 26,79 (0.03) |
| normal potato | 32.1 (0.6) | 19.5 | 28.2 (0.4) | 27.41 (0.05) |
| HAP potato | 73.1 (1.5) | 38.5 | 57 (2) | 29.5 (0.6) |
| *C. zedoaria* | 63.8[d] | 18.8 | 33.5 (0.3) | 28.50 (0.3) |

[a] Annotations as in Table 1. SE in parentheses. [b] Determined by enzyme linked assay. [c] Determined by ICP-AES. [d] Mean of duplicate.

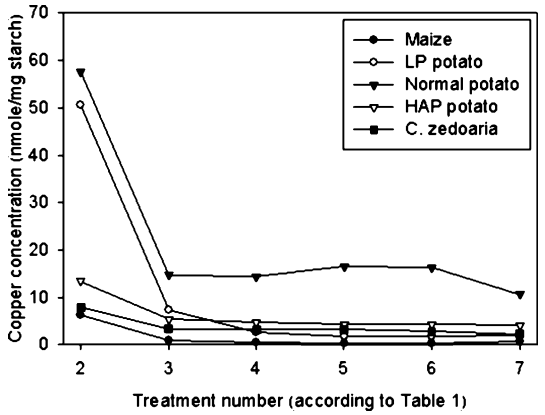


**Figure 1.** Concentration of $Cu^{2+}$ ions in the starch samples, obtained by ICP-AES, as a function of equilibration with water (Table 1).

To permit EPR analysis providing information about interactive sites of the different starch granule matrices, the different starch types were doped with $Cu^{2+}$ ions. In the samples washed with diluted acid and then neutralized (sample no. 1) no copper was detected by ICP-AES. Sample no. 2, obtained by impregnation of the appropriate acid washed starch with 1 M $CuCl_2$ solution followed by equilibration only once with water (10 mL/1 g of starch), revealed the highest content of copper. Stepwise equilibration with water decreased the concentration of copper in the starch granules to constant levels depending on the starch type (Figure 1). Interestingly, the molar ratio between copper and phosphate was significantly lower than unity (Figure 1 and Table 2), especially for the *C. zedoaria* and the HAP starch granules, suggesting that the majority of the phosphate groups are still in the protonized form. This indicates that most of the phosphate groups were unavailable for direct interaction with the copper ions. The normal potato starch contained the highest concentration of copper indicating the presence of a higher concentration of exposed phosphate groups and/or a presence of copper bound in a different way Thus, the EPR data interpreted as a result of phosphate copper interactions described in the next coming sections are specifically represented by the fraction of phosphate groups exposed to interaction with copper ions.

**EPR Spectra of Copper Complexes with Starch.** Before impregnation with the $CuCl_2$ solution (sample no. 1) the starch

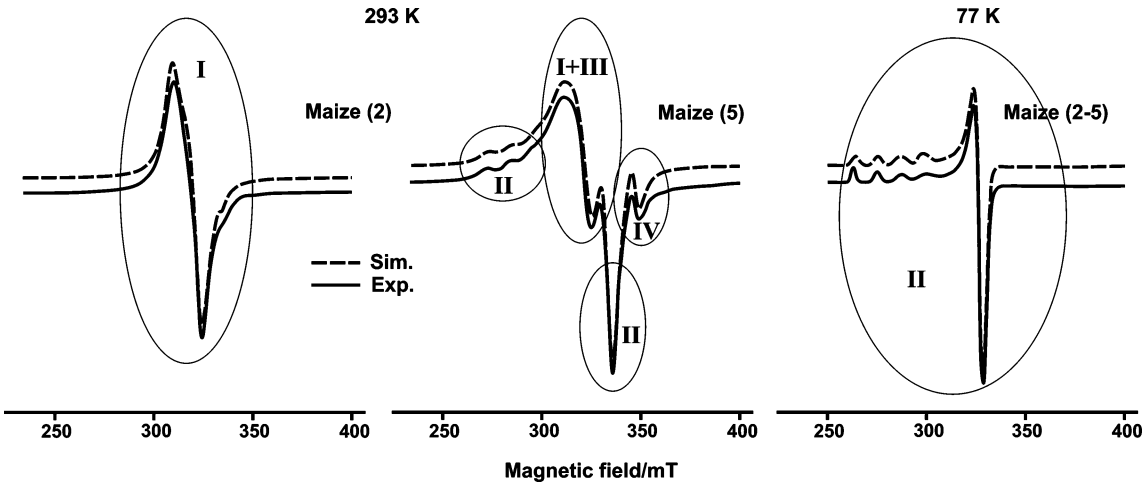


**Figure 2.** Experimental and simulated EPR spectra of $Cu^{2+}$ complexes in maize, registered at 293 and 77 K after several steps of washing. Ellipses indicate areas in which particular component signals (from Figure 7) are dominating.

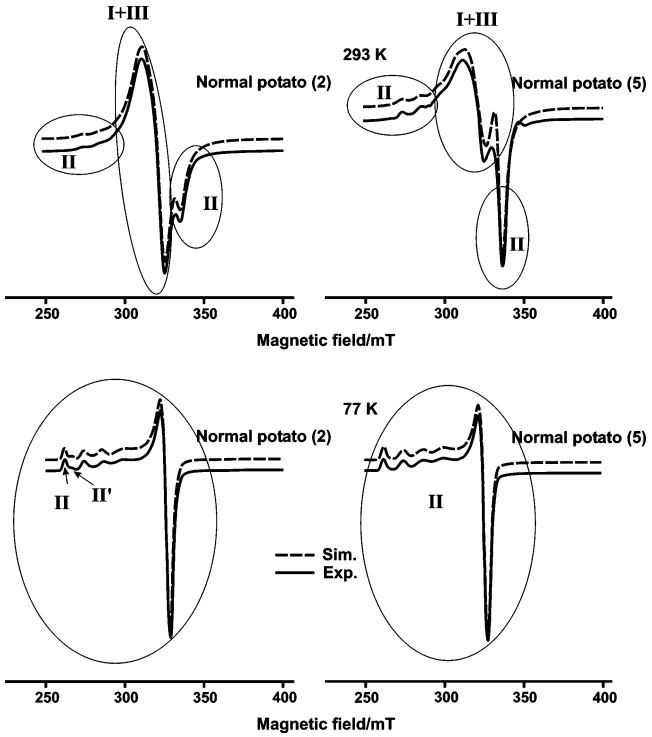


**Figure 3.** Experimental and simulated EPR spectra of $Cu^{2+}$ complexes in normal potato starch, registered at 293 and 77 K after several steps of washing. Ellipses indicate areas in which particular component signals (from Figure 7) are dominating.

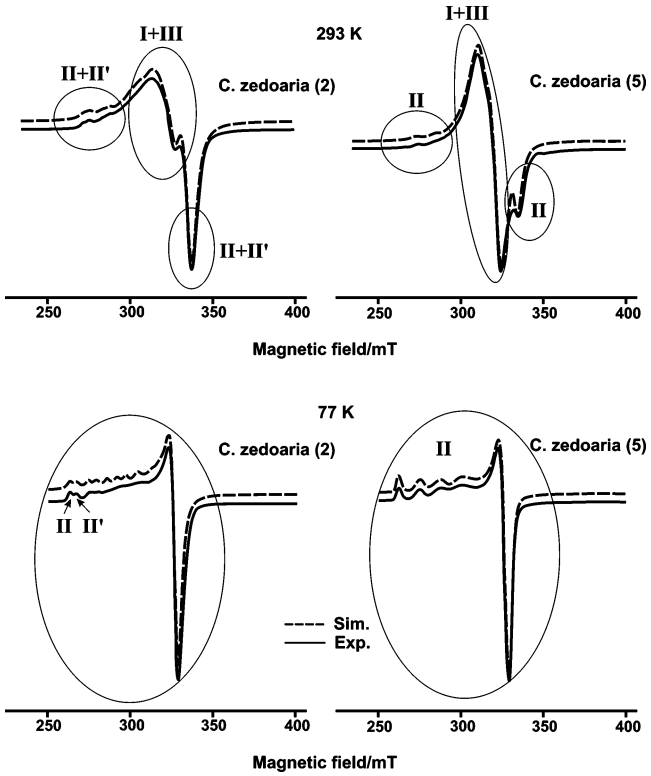


**Figure 4.** Experimental and simulated EPR spectra of $Cu^{2+}$ complexes in *C. zedoaria* starch, registered at 293 and 77 K after several steps of washing. Ellipses indicate areas in which particular component signals (from Figure 7) are dominating.

samples did not exhibit any EPR signal. Following impregnation with 1 M $Cu^{2+}$ ions and one water equilibration (sample no. 2), complex EPR spectra were observed at room temperature and 77 K, indicating formation of several specific copper adducts with the starch matrix. In Figures 2−4, EPR spectra of representative samples containing different amounts of phosphate - maize, normal potato, and *C. zedoaria* - registered at 293 and 77 K, together with simulated ones, after several steps of equilibration (sample nos. 2−5), are presented. The spectra differ strongly in their shape, EPR parameters of particular signals, relative intensity, and relaxation characteristics, depending on the type of the starch, concentration of phosphate, and content of $Cu^{2+}$ ions. Hence, the starch matrices show considerable differences depending on the molecular structures generated by the different starch crop genotypes. Interpretation of these spectra with regard to molecular structures of the different types of starch granules requires quantification of intensity, simulation to generate sub spectral components, and analysis of additional chemically and physically treated starch models with specific structural properties. Such data are provided in the following sections of this work.

The total intensities of the spectra registered at room temperature as a function of consecutive equilibrations with water are presented in Figure 5. For sample no. 2, after impregnation with $Cu^{2+}$ followed by the first equilibration with water, the intensities of the signals are the highest. They are of the order of $5 \times 10^{18}$ spins/g (10 nmol/mg starch), i.e., about five times less than the total content of copper (II) determined analytically for normal potato and LP potato. Upon further equilibrations, signal intensities decrease most distinctly (30−40 times) for maize and LP potato, containing the smallest

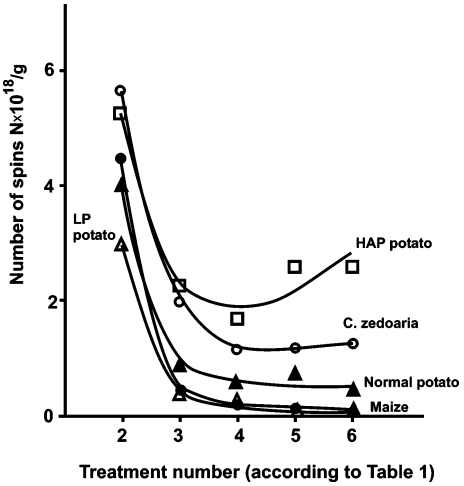


**Figure 5.** Number of spins/g calculated from the EPR spectra (registered at 293 K) of $Cu^{2+}$ complexes in various types of starch after consecutive steps of equilibration with water.

amount of phosphate. In the phosphate rich samples nos. 4−5, stabilization of signal intensities occurs at the level of $2 \times 10^{18}$ spins/g; thus, they are only about 2.5 times smaller than in the initial samples.

The number of spins per one gram of the samples equilibrated 3−5 times increases with increasing content of phosphate and becomes the highest for HAP potato and *C. zedoaria*. This relation proves that there is a significant influence of phosphate on the number of paramagnetic copper adducts formed with the starch matrix.

Comparison of the analytical and EPR data indicates that in all of the investigated samples no. 2 the amount of copper (II) detectable by EPR is smaller than that determined by ICP-AES method. The reason for such discrepancy may be the presence of clustered $Cu^{2+}$ ions, not seen in the EPR spectra due to the strong antiferromagnetic coupling.[43] Such species are weakly bound to the starch matrix or even can form separate phases and, particularly in the case of the samples LP potato containing the smallest amount of phosphate, can be easily removed by equilibration with water (Figure 1).

Total EPR signal intensities increased upon lowering the temperature from 293 to 77 K (Figure 6). After stabilization (sample nos. 4−5), the ratio $I_{77}/I_{293}$ (where $I_T$ is the total signal intensity at temperature T/K) for all of the samples is equal to about 4.0, indicating the presence of paramagnetic behavior of the copper complexes, according to the Curie−Weiss law. However, for sample no. 2 of maize, the ratio is equal to 3.0, indicating the existence in this sample of some copper complexes with antiferromagnetic interactions,[43] i.e., weakly bound, clustered, and EPR silent copper species.

The various types of the starch containing copper show at room temperature complex spectra consisting of three main signals (Figure 7, signals I, II, and III) present in various proportions. Moreover, signal IV was detected in starches with a small content of phosphate and in the lintnerised starches, i.e., starch granules where the amorphous parts have been selectively removed by hydrolysis. This effect will be discussed later. The spectra of all of the samples registered at 77 K were very similar (Figure 7, signal $II_{77}$ and $II'_{77}$). The relative concentrations of the particular components in different samples of the starch and their changes upon equilibration with added water are presented in Figure 8.

Signal I is visible at room temperature in the spectra of all samples, which were equilibrated only once with water. It

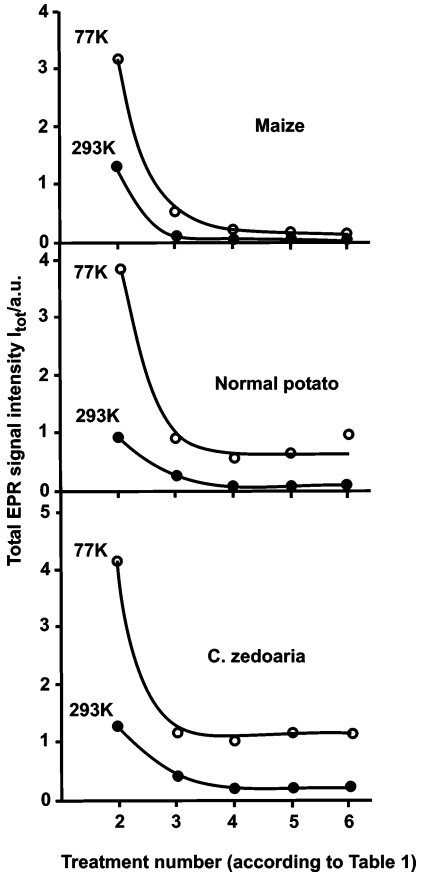


**Figure 6.** Comparison of the total integral EPR signal intensities, registered at 293 and 77 K, for representative types of starch after consecutive steps of equilibration with water.

exhibits, depending on the kind of starch, the following parameters: $g_{\|} = 2.252-2.323$ and $g_{\perp} = 2.140-2.228$. Signal I loses its intensity upon lowering the temperature, and at 77 K the species responsible for it became mostly EPR silent (Figure 6). Such behavior indicates the existence of exchange interactions of antiferromagnetic type between paramagnetic centers. Indeed, the value of parameter $G = (g_{\|} - g_e)/(g_{\perp} - g_e)$, which is a measure of exchange interactions,[44] is equal to 1.3−1.6, confirming the strong coupling between $Cu^{2+}$ species. Signal I is present in the EPR spectra of all samples, but it dominates in the spectrum of maize (Figure 8, sample no. 2). Species responsible for this signal are easily removed by equilibration with excess water (Figure 8, sample nos. 3−5) which means that they are located in the well accessible fractions of the starch matrix. We ascribe signal I to clustered copper centers situated on the surfaces of the starch granule, easily reached by water. Such surfaces can exist in amorphous parts of the starch within the branch point lamellae and/or in amylose rich volumes. Indeed, signal I is absent in the highly crystalline Lintner starches, what confirms its attribution to the amorphous regions only (see section *Evolution of EPR Spectra from Modified Starch*). Since starch granules can be penetrated by molecules as large as 1000 Da,[45] such surfaces can be internal as well as external. The procedure of drying the starch at 393 K for 2 h (see section *Evolution of EPR Spectra from Modified Starch*) leads to the disappearance of signal I, which may be caused by the increase of dipolar and/or exchange interactions between $Cu^{2+}$ ions completely devoid of water molecules. Similar signals of clustered $Cu^{2+}$ ions were observed in montmorillonites, and they were also attributed to strongly interacting copper centers.[46]

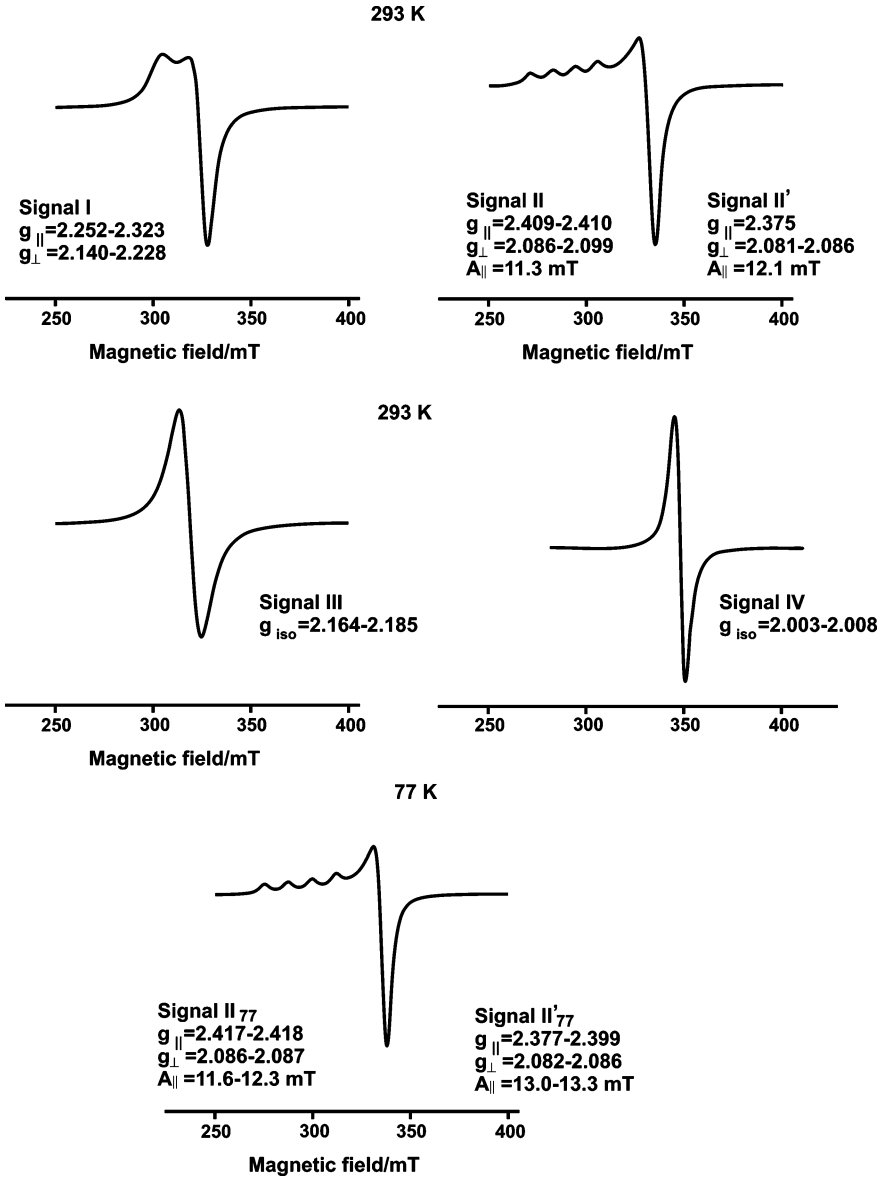


**Figure 7.** Particular components of the spectra of $Cu^{2+}$ complexes in starch registered at 293 K and at 77 K, found by simulation procedure.

The equilibration procedure leads to the decrease in the intensity of signal I while the other components of the EPR spectrum become simultaneously more visible (Figure 8). All starches exhibited at room temperature an anisotropic signal, signal II, with clearly defined $g_{||}$ and $g_{\perp}$ values (Figure 7). The well resolved four-line hyperfine structure (HFS) around $g_{||}$, due to the interactions of the unpaired electron with $^{63,65}Cu$ nuclei ($I = 3/2$), confirmed the existence of isolated $Cu^{2+}$ centers. The width of the components of the HFS increased with increasing magnetic field, i.e., with increasing quantum number $m_S = -3/2, -1/2, 1/2$, and $3/2$ responsible for a given transition. Such broadening of the HFS lines can be attributed to the inhomogeneity of the crystal field surrounding copper ions[47] in the starch matrix. The perpendicular features of the HFS remain unresolved. The dependence of $g_{||} > g_{\perp} > g_e$, observed for this signal, indicates axial symmetry of the copper species with $d_{x^2-y^2}$ ground state of $Cu^{2+}$.[48] The $g$ tensor components for such symmetry are related with the ligand field parameters by formulas: $\Delta g_{||} = g_{||} - g_e = -8\lambda/\Delta$ and $\Delta g_{\perp} = g_{\perp} - g_e = -2\lambda/\delta$, where $g_e$ is the free electron $g$ value, $\lambda$ is the spin−orbit coupling constant equal to $-821$ cm$^{-1}$, and $\Delta$ and $\delta$ are energies of the splitting of orbital levels by the crystal field. The values of $\Delta = E(d_{x^2-y^2} - d_{xy})$ and $\delta = E(d_{x^2-y^2} - d_{xz,yz})$ are attributed to the optical transitions $d_{x^2-y^2} \rightarrow d_{xy}$ and $d_{x^2-y^2} \rightarrow d_{xz,yz}$, respectively. The parameters of signal II $g_{||} = 2.409-2.410$, $g_{\perp} = 2.086-2.099$, $A_{||} = 11.3$ mT correspond to the copper ions situated in an elongated octahedron of oxygen ligands.[49] The maize starch granules, which did not contain starch phosphate esters but where the small amounts of phosphate is bound to lipids, showed a type II signal with parameters slightly different ($g_{||} = 2.398$, $g_{\perp} = 2.094$, $A_{||} = 12.1$ mT). The species responsible for signal II are situated in the fraction of the starch granule less accessible to water as indicated by their better resistance to be removed by equilibration with water compared to the species giving signal I (Figure 8).

Starch types rich in phosphate and equilibrated only once with added water showed an additional signal, signal II′, with clearly resolved HFS features (Figure 7). The EPR parameters of this signal ($g_{||} = 2.375$, $g_{\perp} = 2.081-2.086$, $A_{||} = 12.1$ mT) differ somewhat from those of signal II. Particularly, the value of $g_{||}$ component of signal II′ is smaller than that of signal II which pointed to the stronger interaction of $Cu^{2+}$ ion with ligands. The species responsible for signal II′ are easily removed upon equilibration with water. For example, in *C. zedoaria*,

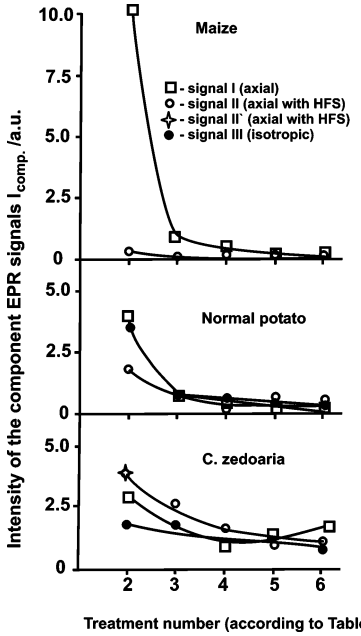


**Figure 8.** Changes in the intensity of the particular component signals, registered at 293 K, for representative types of starch after several steps of equilibration with water, calculated by simulation procedure.

signal II′ was seen only in the sample No 2 and disappeared upon further equilibration (Figure 8). Hence, the reason for the diminishing $g_{||}$ value cannot be increase of the strength of bonding of $Cu^{2+}$ ions with oxygens of the starch matrix but rather change in the type of other ligands. As mentioned in the Introduction, the $CuCl_2$ water solutions used for impregnation of the starch (see *Materials*) contain various $Cu^{2+}$ complexes with water and $Cl^-$ ligands, like $[Cu(H_2O)_2Cl_x]$. The EPR parameters of the latter species differ from those observed for hexaaqua complex of $Cu^{2+}$, i.e., the corresponding $g_{||}$ values are lower. Thus, e.g., for $[Cu(H_2O)_6]^{2+}$ $g_{||} = 2.400$,[50] whereas for $[Cu(H_2O)_2Cl_4]^{2-}$ $g_{||} = 2.380$[51,52] and for $[Cu(H_2O)_2Cl_2]$ $g_{||} = 2.252$.[53] Similarly, $g_{\perp}$ values of signal II′ are smaller than those of signal II. Hence, signal II′ could be ascribed to complexes of $Cu^{2+}$ with $Cl^-$ and $H_2O$ ligands, weakly interacting with the starch matrix.

The third component of the spectra registered at room temperature is an isotropic, relatively broad signal, signal III, with $\Delta B_{pp} = 8.5-15.0$ mT (where $\Delta B_{pp}$ is peak-to-peak width of the first derivative signal) and $g_{av} = 2.164-2.185$ (where $g_{av}$ is average value of the signal) (Figure 7). The parameters of signal III are typical for freely rotating $[Cu(H_2O)_6]^{2+}$ complexes.[54] The fact, that this signal exhibits high intensity in the samples containing phosphate, confirms that the presence of phosphate facilitates binding of water and/or extends the space accessible for rotation of the $[Cu(H_2O)_6]^{2+}$ complexes. After lowering the temperature to 77 K the isotropic signal III is no more present in the EPR spectrum verifying its mobile nature. A signal of copper-starch complex with HFS resolved at room temperature with EPR parameters similar to signal II described above was found by Śmigielska et al.[33] The authors observed also isotropic component of the EPR spectrum, however they attributed this single line not to the free rotating hexaaqua complex $[Cu(H_2O)_6]^{2+}$ but to clustered $Cu^{2+}$ ions. The results of EPR measurements performed in the present work at 77 K and dehydration experiments described in section *Analysis of the Annealed and Dehydrated Samples* speak, however, in favor of our interpretation.

The correlation between starch phosphate and the EPR signal III provides some interesting information on possible effects of phosphate in the granule matrix. EPR signal III, representing freely rotating copper hexaaqua complexes demonstrates the localization of phosphate in hydrated cavities in the starch granule. This data does of course not itself provide evidence for an effect caused by the phosphate group. However, support for a phosphate-induced hydrating effect in the granule matrix comes with X-ray scattering and DSC data[19−21] demonstrating decreased crystallinity and melting enthalpy for phosphorylated starches indicating that the phosphate groups can induce space in the glucan matrix. Our data support this interpretation. Another copper type represented by the well dispersed $Cu^{2+}$−starch complexes with axial symmetry that are less accessible to water (signal II), also correlated with the phosphate concentration, demonstrate the presence of a fraction of phosphate groups more tightly bound to the starch matrix and possibly not extensively hydrated but accessible for interaction with $Cu^{2+}$. The presence of phosphate groups that are completely inaccessible for copper exchange and hence cannot be probed by EPR are supposedly well aligned in crystalline segments in the glucan matrix. The existence of the two latter is further supported by a molecular model generated for phosphorylated double helical starch.[23] Hence our EPR data and our copper ion exchange level data together with X-ray, DSC, and force field molecular modeling support the simultaneous presence of several different phosphate fractions in the starch granules and that one of these fractions possible create hydrated cavities in the starch granule matrix.

At 77 K, the EPR spectra of the all types of the starch consisted only of the axial signals exhibiting well resolved HFS (Figures 2-4 and 7). Several samples containing phosphate equilibrated only once or twice with water gave at 77 K, similarly as at room temperature, two component spectra with the signals $II_{77}$ and $II'_{77}$ exhibiting the following parameters:

signal $II_{77}$: $g_{||} = 2.417-2.418$, $g_{\perp} = 2.086-2.087$, $A_{||} = 11.6-12.3$ mT

signal $II'_{77}$: $g_{||} = 2.377-2.399$, $g_{\perp} = 2.082-2.086$, $A_{||} = 13.0-13.3$ mT

The equilibration procedure leads to the disappearance of signal $II'_{77}$ in the spectra registered at 77 K, and only signal $II_{77}$ was observed for all starch types, independently of washing with water.

The parameters of signal II at 77 K differ from those at the room temperature and are similar to those found at the same temperature for copper species in zeolites and montmorillonites [46,54,55] as well as in synthetic polymers[31] which were ascribed to hexacoordinated $[Cu(H_2O)_6]^{2+}$ complexes. Hence, signal $II_{77}$ is probably a result of overlapping of two independent signals: one assigned to the species $[Cu(H_2O)_6]^{2+}$ freely rotating and giving signal III at room temperature and signal II with HFS resolved at room temperature. This topic will be discussed in detail later on (see section *Evolution of EPR Spectra from Modified Starch)*.

Spectra of some starches with small and medium content of phosphate: maize, LP potato, and normal potato exhibit additionally a narrow, isotropic signal, signal IV, with *g* factor equal to 2.003−2.008 (Figure 2, 3, and 7). The EPR parameters of signal IV are similar to those of radicals formed in the starch by thermal treatment[29,30] or by irradiation.[27]

**Evolution of EPR Spectra from Modified Starch (Lintnerisation and Dehydration).** *Analysis of Lintner Starches.* The

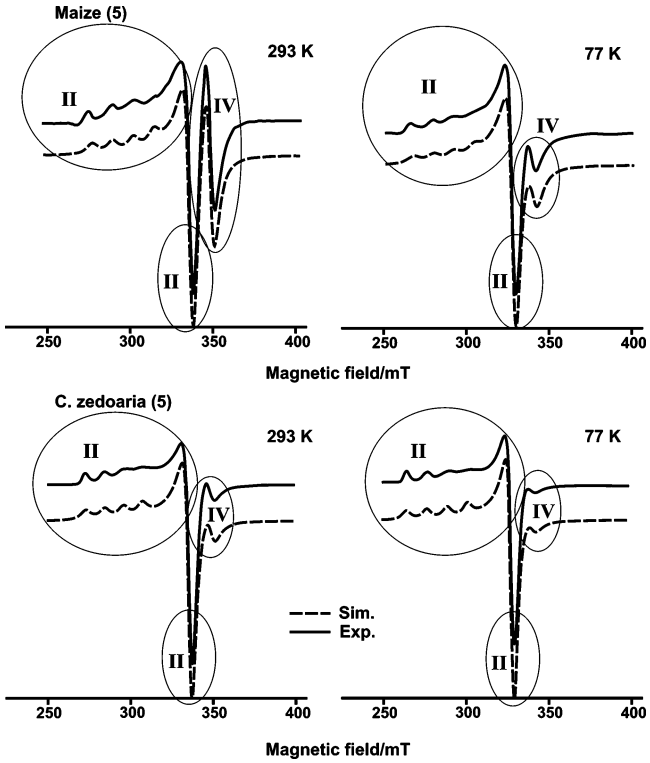


**Figure 9.** Experimental and simulated EPR spectra of the Lintner starches: maize and *C. zedoaria* registered at 293 and 77 K. Signal IV is related to the radical species located in the crystalline fraction of the starches. Ellipses indicate areas in which particular component signals (from Figure 7) are dominating.

**Table 3.** EPR Parameters of the Copper Complexes in Lintnerised Starch Granules

| sample registration temp. | maize 293 K | maize 77 K | normal potato 293 K | normal potato 77 K | *C. zedoaria* 293 K | *C. zedoaria* 77 K |
|---|---|---|---|---|---|---|
| $g_{\|\|}$ | 2.364 | 2.377 | 2.400 | 2.406 | 2.410 | 2.414 |
| $g_{\perp}$ | 2.083 | 2.079 | 2.087 | 2.085 | 2.086 | 2.084 |
| $A_{\|\|}$/mT | 12.4 | 12.7 | 12.6 | 12.8 | 11.4 | 12.3 |
| $\Delta$/cm$^{-1}$ | 18 345 | 17 705 | 16 700 | 16 430 | 16 265 | 16 035 |
| $\delta$/cm$^{-1}$ | 20 610 | 21 690 | 19 610 | 20 110 | 19 750 | 20 185 |

procedure of lintnerisation leading to the removal of the amylose and the amorphous amylopectin fractions from the starch granule has a significant influence on the EPR spectra of the all investigated starches. After hydrolysis, the spectra of all kinds of starch consist only of the main signal II exhibiting the HFS and signal IV (Figure 9). The remaining signals I and III disappear completely from the EPR spectra confirming that they are connected with the amorphous or nonhelical regions of the starch granule matrix. As mentioned above, the intensity of signal IV decreases upon increase of the phosphate content, and hence, its localization in the crystalline fraction of the starch impoverished in phosphate is confirmed.

The parameters of signals II observed in Lintners of maize starch not containing phosphate covalently esterified to the starch molecules differ from those for phosphorylated specimens (normal potato and *C. zedoaria*, Table 3) indicating different surroundings of $Cu^{2+}$ ions in both kinds of starches. The presence of phosphate leads to the significant increase in both $g_{\|}$ and $g_{\perp}$ values in comparison to maize. The crystal field parameters calculated for these species clearly indicate weakening of the crystal field around the copper center in the starch containing phosphate.

Binding of $Cu^{2+}$ ions to the starch matrix consists on replacement of some $H_2O$ ligands in the coordination sphere of hexaaqua complex by −O−C− and/or −O−P− functional groups of the starch structure originating from free hydroxyl groups of the anhydrous glucose and phosphate units. Replacement of $H_2O$ ligands by −O−P− functional groups, occurring mainly in the samples with high content of phosphorus, consists of change of H into P atoms in the outer coordination sphere of $Cu^{2+}$. Both elements (H and P) have similar values of electronegativity (2.20 and 2.19, respectively[56]). Hence, the EPR parameters of the corresponding Cu complexes should not change considerably.

On the other hand, introduction of ligands with higher electronegativity into the outer coordination sphere of copper−oxygen species causes decrease of $g_{\|}$ value, as shown, e.g., by Wells et al. and Koga and Hukuda.[57] This change indicates increase of interactions between the central atom and ligands. Similar effects were observed in the investigated $Cu^{2+}$−starch complexes. Carbon has a much higher value of electronegativity (equal to 2.55[56]) than H and P. Indeed, the data in Table 3 indicate that maize (with very small content of P) exhibits smaller value of $g_{\|}$ than those observed in phosphorylated starches, because of the higher electronegativity of carbon which is an outer ligand, $[-C-O-Cu(H_2O)_n]$, in the maize structure. These results indicate weaker interactions of $Cu^{2+}$ central ion with terminal −O−P− groups than with −O−C− groups in the starch matrix, confirmed additionally by lower value of $A_{\|}$ as found in the highly phosphorylated *C. zedoaria* starch (Table 3). Hence, specific $Cu^{2+}$ phosphate interaction in a hydrated environment is strongly indicated.

It is worthwhile to note that $g$ factor values change with decreasing temperature. In all cases, the $g_{\|}$ parameter increased whereas the value of $g_{\perp}$ decreased. Such changes can be connected with a change of the structure of $Cu^{2+}$ centers upon lowering the temperature, e.g., flattening of the $CuO_6$ octahedra.

Taking into account that signal II present in the lintnerised starch granules is related to a single copper species only, i.e., to that bound to the starch matrix, subtraction of this signal registered at 77 K from the EPR spectrum of the native starch (amylopectin + amylose) containing at the same temperature two components: signal II and signal III, allow the EPR parameters of signal III to be estimated at 77 K. For all investigated starches, the parameters of signal III attributed to the $[Cu(H_2O)_6]^{2+}$ complex, rotating at 293 K and immobilized at low temperature, found by this method, were practically the same ($g_{\|} = 2.427-2.429$, $g_{\perp} = 2.088-2.090$, $A_{\|} = 11.4-12.1$ mT) confirming correctness of the applied procedure.

*Analysis of the Annealed and Dehydrated Starches.* The treatment of starch granules in aqueous media at temperatures just below the gelatinization temperature leads to increased ordering of the double helical crystalline arrays forming the crystalline part of the starch granule matrix.[58] For these starches, changes in the EPR spectra were observed, especially of starches containing phosphate. Comparison of the EPR spectrum of *C. zedoaria* equilibrated five times (sample no. 5) with corresponding annealed sample (sample no. 6) indicates that upon annealing the contribution of signal III, connected with the complex $[Cu(H_2O)_6]^{2+}$, decreases, confirming the contribution of this signal to increased ordering of double-helical glucan structures following the annealing procedure. The amount of species related with signal II does not change, indicating that they are not susceptible to annealing treatment. On the other hand, the intensity of signal I increases. Since annealing preferentially induces a registration of unordered double helical segments into crystalline arrays, these data suggest an annealing-dependent transformation of phosphate groups residing as

complex $[Cu(H_2O)_6]^{2+}$ (species III) in double-helical, but unordered, starch sections into clustered copper complexes (signal I) in ordered double helical segments.

Complete dehydration of starch granules producing substantially decreased amounts of crystalline glucan structures[59] leads to more drastic changes in the EPR spectra. After drying at 393 K for 2 h not only signal III, but also signal I, ascribed to clustered copper complexes, disappears. Vanishing of the latter signal following the dehydration procedure, leading to removal of water molecules from the coordination sphere of $Cu^{2+}$, is supposedly an effect of increased dipolar and/or exchange interactions between copper ions resulting in the significant broadening of the signals and their partial elimination from the EPR spectra.

## Conclusions

The EPR study of the different starch types generated using a transgenic approach, with $Cu^{2+}$ ions as a paramagnetic probe, revealed formation of several specific copper species, bound to the starch matrix with different strength, depending on the concentration of phosphate as well as the molecular and general conformational properties of the starch matrix. Hence, the data provides information about the effects of specific gene products, GBSS, SBE, and GWD on the starch granule assembly process. Investigation of the native and Lintner starches allowed to distinguish between species located in amorphous amylose and semicrystalline amylopectin fractions. Copper adducts were identified, two of which were found to be linked with starch phosphate groups. However, it is emphasized that large fractions of the phosphate groups in the starch matrices were not at all exposed for interaction with the copper ions indicating a dense environment around these phosphate groups.

The following types of copper adducts were found in the amorphous fraction of the starch:

(1) Cu complexes with axial symmetry, coupled by antiferromagnetic interactions (signal I), weakly bound to the starch matrix. These species are easily accessible to water and situated most probably on surfaces of the starch granules. The relative amount of these species is the highest in maize before repeated equilibration with water and decreases upon introduction of phosphate.

(2) Hexaaqua complexes of copper (signal III), freely rotating at room temperature and immobilized at 77 K, formed mainly in starches containing phosphate. Together with X-ray and DSC data this fact substantiates that a fraction of the phosphate groups can facilitate binding of water and/or creates hydrated space in the starch granule matrix.

In the semicrystalline fraction of the starch the following complexes are formed:

(1) Well dispersed $Cu^{2+}$−starch complexes with axial symmetry (signal II), less accessible to water than the species related with signal I. In the starches of low phosphate content the $Cu^{2+}$ species II are linked to the starch matrix by −O−C− groups whereas in phosphorylated starches mainly by −O−P− bonds, supposedly phosphate groups located in crystalline domains. With increasing content of phosphate the amount of these species increases.

(2) Radical species exhibiting a narrow, isotropic signal (signal IV), the amount of which is reduced by the presence of phosphate groups and supposedly located in highly crystalline starch fractions.

**Acknowledgment.** Per Lassen Nielsen is acknowledged for technical assistance. Maize starch was a kind gift from Cerestar AKV Langholt, Denmark. The authors (E.B., K.D., and M.Ł.) gratefully acknowledge partial financing of the work from the Grant No. 2 PO6T 087 27 awarded by the Polish Ministry of Science and Informatics. A.B. and K.H. acknowledge The Danish National Research Foundation, The Danish Biotechnology Program, the Danish Directorate for Development (Centre for Development of Improved Food Starches) and The Commitee for Research and Development of the Öresund Region (Öforsk) for financial support.

## References and Notes

(1) Ellis, R. P.; Cochrane, M. P.; Dale, M. F. D.; Duffus, C. M.; Lynn, S.; Morrison, I. M.; Prentice, R. D. M.; Swanston, J. S.; Tiller, S. A. *J. Sci. Food Sci.* **1998**, *77*, 289−311.
(2) Gallant, D. J.; Bouchet, B.; Baldwin, P. M. *Carbohydr. Polym*. **1997**, *32*, 177−191.
(3) Waigh, T. A.; Gidley, M. J.; Komanshek, B. U.; Donald A. M. *Macromolecules* **1998**, *31*, 7980−7984.
(4) Imberty, A.; Chanzy, H.; Pérez, S.; Buléon, A.; Tran, V. *J. Mol. Biol.* **1988**, *201*, 365−378.
(5) Imberty, A.; Pérez, S. *Biopolymers* **1988**, *27*, 1205−1221.
(6) Blennow, A.; Engelsen, S. B.; Nielsen, T. H.; Baunsgaard, L.; Mikkelsen, R. *Trends Plant Sci.* **2002**, *7* (9), 445−450.
(7) Blennow, A.; Engelsen, S. B.; Munck, L.; Møller, B. L. *Carbohydr. Polym*. **2000**, *41*, 163−174.
(8) Tabata, S. Nagata, K.; Hizukuri, S. *Starch/Stärke* **1975**, *27*, 333−335.
(9) Samec, M. *Kolloidchem. Beih.* **1914**, *4*, 2−54.
(10) Posternak, T. *Helv. Chim. Acta* **1935**, *18*, 1351−1369.
(11) Bay-Smidt, A. M. Wischmann, B. Olsen, C. E.; Nielsen, T. H. *Starch/Stärke* **1994**, *46*, 167−172.
(12) Hizukuri, S.; Tabata, S.; Nikuni, Z. *Starch/Stärke* **1970**, *22*, 338−343.
(13) Tabata, S.; Hizukuri, S. *Starch/Stärke* **1971**, *23*, 267−272.
(14) Blennow, A.; Bay-Smidt, A. M.; Wischmann, B.; Olsen, C. E.; Møller, B. L. *Carbohydr. Res.* **1998**, *307*, 45−54.
(15) Takeda, Y.; Hizukuri, S. *Carbohydr. Res.* **1982**, *102*, 321−327.
(16) Mikkelsen, R.; Baunsgaard, L.; Blennow, A. *Biochem. J.* **2004**, *377* (2) 525−532.
(17) Blennow, A.; Sjöland, K. A.; Andersson, R.; Kristiansson, P. *Anal. Biochem.* **2005**, in press.
(18) Blennow, A.; Bay-Smidt, A. M. Olsen, C. A.; Møller, B. L. *Int. J. Biol. Macromol.* **2000b**, *27*, 211−218.
(19) Muhrbeck, P.; Eliasson, A.-C. *J. Sci. Food Agric.* **1991**, *55*, 13−18.
(20) Kim, Y. P. Wiesenborn, D. P.; Orr, P. H.; Grant, L. A *J. Food Sci. Agric*. **1995**, *60*, 1060−1065.
(21) Muhrbeck, P. Svensson, E.; Eliasson, A.-C. *Starch/Stärke* **1991**, *43*, 466−468.
(22) O'Sullivan, A. C.; Perez, S. *Biopolymers* **1999**, *50*, 381−390.
(23) Engelsen, S. B.; Madsen, M. A. O.; Blennow, A.; Motawia, S.; Møller, B. L.; Larsen, S. *FEBS Lett.* **2003**, *541*, 137−144.
(24) Kossmann, J.; Lloyd, J. *Crit. Rev. Plant Sci.* **2000**, *19*, 171−226.
(25) Viksø-Nielsen, A.; Blennow, A.; Jørgensen, K.; Kristensen, K. H.; Jensen, A.; Møller, B. L. *Biomacromolecules* **2001**, *3*, 836−841.
(26) Wiesenborn, D. P. Orr, P. H. Casper, H. H.; Tacke. B. K. *J. Food Sci.* **1994**, 59 3, 644−648.
(27) Bertolini, A. C.; Mestres, C.; Colonna, P.; Raffi, J. *Carbohydr. Polym.* **2001**, *44*, 269−271.
(28) Merlin, A.; Fouassier, J. P. *Macromol. Chem.: Macromol. Symp.* **1981**, 3053−3068.
(29) Ciesielski, W.; Tomasik, P. *Carbohydr. Polym*. **1996**, *31*, 205−210.
(30) Bidzińska, E.; Dyrek, K.; Fortuna, T.; Łabanowska, M.; Pietrzyk, S. *Starch/Stärke* **2004**, *56*, 461−468.
(31) Kruczała, K.; Schlick, S. *J. Phys. Chem. B* **1999**, *103*, 1934−1943.
(32) Ciesielski, W.; Lii, Ch.; Yen, M.-T.; Tomasik, P. *Carbohydr. Polym.* **2003**, *51*, 47−56.
(33) Śmigielska, H.; Lewandowicz, G.; Goslar, J.; Hoffmann, S. K. *Acta Phys. Polon. A* **2005**, *108*, 303−310.
(34) Blennow, A.; Wischmann, B.; Houborg, K.; Ahmt T.; Madsen, F.; Poulsen, P.; Jørgensen, K.; Bandsholm, O. *Int. J. Biol. Macromol*. **2005**, *36*, 159−168.
(35) Wischmann, B.; Blennow, A.; Madsen, F.; Jørgensen, K.; Poulsen, P.; Bandsholm, O. *Food Hydrocolloids* **2005**, in press.
(36) Jane, J.-L.; Wong, K. S.; McPherson, A. E. *Carbohydr. Res.* **1997**, *300*, 219−227.
(37) Muhrbeck, P.; Wischmann, B. *Starch/Stärke* **1998**, *50*, 423−426.

(38) Dyrek, K.; Madej, A.; Mazur, E.; Rokosz A. *Colloids Surf.* **1990**, *45*, 135−144.
(39) Dyrek, K.; Rokosz, A.; Madej, A. *Appl. Magn. Reson.* **1994**, *6*, 309−332.
(40) Dyrek, K.; Bidzińska, E.; Adamski, A. *Mol. Phys. Rep.* **2003**, *29*, 793−804.
(41) SIM14 Program, QCPE No 265.
(42) Łagan, J. M. Jagiellonian University, Cracow, Poland, 1991, unpublished data.
(43) Solomon, E. I. *Pure Appl. Chem.* **1983**, *55* (7), 1069−1088.
(44) Hathaway, B. J. *J. Chem. Soc., Dalton* **1972**, 1196−1199.
(45) Planchot, V.; Roger, P.; Colonna, P. *Starch/Stärke* **2000**, *52*, 333−339.
(46) Bahranowski, K.; Dula, R.; Łabanowska, M.; Serwicka, E. M. *Appl. Spectrosc.* **1996**, *50*, 1439−1445.
(47) Hasono, H.; Kawazoe, H.; Kanazawa, T. *J. Non-Cryst. Solids* **1979**, *33*, 103−115.
(48) Abragam, A., Bleaney, B., Eds.; *Electron Paramagnetic Resonance of Transition Metal Ions*; Dover Publications: New York, 1986.
(49) Atanasov, M.; Petrov, K.; Mirtcheva, E. *J. Sol. State Chem.* **1995**, *118*, 303−312.
(50) Lewis, W. B.; Alei, M.; Morgan, L. O. *J. Chem. Phys.* **1966**, *45*, 4003−4013.
(51) Abe, H.; Ono, K.; Hayashi, I.; Shimada, J.; Iwanaga, K. *J. Phys. Soc. Jpn.* **1954**, *9*, 814−822.
(52) Ono, K.; Ohtsuka, M. *J. Phys. Soc. Jpn.* **1958**, *13*, 206−209.
(53) Gerritsen, H. J.; Bolger, B.; Okkes, R. F. *Rep. Prog. Phys.* **1955**, *18*, 304.
(54) Conesa, J. C.; Soria, J. *J. Chem. Soc., Faraday Trans.* **1979**, *I*, 75, 406−422.
(55) Goslar, J.; Więckowski, A. B. *J. Sol. State Chem.* **1985**, *56*, 101−115.
(56) Pauling, L. *The Nature of the Chemical Bond*; Cornell University Press: Ithaca, New York, 1960.
(57) Goodman, B. A.; Raynor, J. B. *Adv. Inorg. Chem. Radiochem.* **1970**, *13*, 135−362 and references within.
(58) Tester, R. F.; Debon, S. J. J. *Int. J. Biol. Macromol.* **2000**, *27* (1), 1−12.
(59) Lemke, H.; Burghammer, M.; Flot, D.; Rössle, M.; Riekel, C. *Biomacromolecules* **2004**, *5*, 1316−1324.

BM050919G